JRC 2018-6209

IMPACT OF HYSTERESIS HEATING OF RAILROAD BEARING THERMOPLASTIC ELASTOMER SUSPENSION PAD ON RAILROAD BEARING THERMAL MANAGEMENT

Oscar O. Rodriguez
Mechanical Engineering Department
The University of Texas Rio Grande Valley
Edinburg, TX, 78539, USA
oscar.o.rodriguez01@utrgv.edu

Arturo A. Fuentes, Ph.D.
Mechanical Engineering Department
The University of Texas Rio Grande Valley
Edinburg, TX, 78539, USA
arturo.fuentes@utrgv.edu

Constantine Tarawneh, Ph.D.
Mechanical Engineering Department
The University of Texas Rio Grande Valley
Edinburg, TX, 78539, USA
constantine.tarawneh@utrgv.edu

ABSTRACT

It is a known fact that polymers and all other materials develop hysteresis heating due to the viscoelastic response or internal friction. The hysteresis or phase lag occurs when cyclic loading is applied leading to the dissipation of mechanical energy. The hysteresis heating is induced by the internal heat generation of the material, which occurs at the molecular level as it is being disturbed cyclically. Understanding the hysteresis heating of the railroad bearing elastomer suspension element during operation is essential to predict its dynamic response and structural integrity, as well as to predict the thermal behavior of the railroad bearing assembly. The main purpose of this ongoing study is to investigate the effect of the internal heat generation in the thermoplastic elastomer suspension element on the thermal behavior of the railroad bearing assembly. This paper presents an experimentally validated finite element thermal model that can be used to obtain temperature distribution maps of complete bearing assemblies in service conditions. The commercial software package ALGOR 20.3™ is used to conduct the thermal finite element analysis. Different internal heating scenarios are simulated with the purpose of determining the bearing suspension element and bearing assembly temperature distributions during normal and abnormal operation conditions. Preliminary results show that a combination of the ambient temperature, bearing temperature, and frequency of loading can produce elastomer pad temperature increases above ambient of up to 125ºC when no thermal runway is present. The higher temperature increase occurs at higher loading frequencies such as 50 Hz, thus, allowing the internal heat generation to significantly impact the temperature distribution of the suspension pad. This paper provides several thermal maps depicting normal and abnormal operation conditions and discusses the overall thermal management of the railroad bearing assembly.

INTRODUCTION

Reliable health monitoring of railroad bearings is essential to ensure the safe transport of commodities and goods, and to prevent catastrophic failures in the railroad industry. Between 2010 and 2016, there have been approximately 106 freight train derailments that have been caused by the overheating of a bearing in one or multiple railcars [1]. To identify distressed bearings in service, conventional railroad bearing health monitoring systems rely on the bearing cup (outer ring) temperature as detected by wayside monitoring systems, spaced at specific distances alongside tracks, to warn of impending failure. Railroad bearing temperatures are monitored by wayside devices called hot-box detectors (HBDs), which use infrared sensors to take snapshots of bearing temperatures as they pass over the detectors to identify bearings that are operating at temperatures greater than 94.4ºC (170ºF) above ambient conditions [2]. Currently, most U.S. railroads tend to track the temperature of each bearing and compare it to the average temperature of all bearings on the same side of the train. Hence,

bearings that are "trending" above normal can be identified without waiting for a hot-box detector to be triggered [3]. Railroad bearings that are found to be hot are removed from service for later disassembly and inspection. Generally, the overheating of the bearing can be correlated back to one or more of the common modes of bearing failure such as water or dirt contamination, spalling, broken internal components, damaged seals, improper lubrication, etc. However, in many cases, the hot bearings that are set out do not exhibit signs of any of the common causes (i.e. non-verified bearings). Researchers continue to place strong emphasis on issues such as the warm trending phenomenon that leads to the unnecessary and costly removal of non-verified bearings. These temperature health monitoring systems, such as the wayside hot-box detectors (HBDs), have helped to reduce the number of freight train derailments significantly since their implementation. However, their limited accuracy prevents them from being a true continuous health monitoring system. New technologies are focusing on a more frequent (i.e. continuous) method to track temperatures of railroad bearings.

Since placing sensors directly on the bearing is not practical due to cup indexing during service, the next logical location for such sensors is the bearing adapter [4]. The railroad bearing AdapterPlus™, which has replaced many conventional all metal bearing adapters, utilizes the thermoplastic elastomer suspension pad, as shown in Figure 1. The purpose of the elastomer pad is to prevent metal to metal contact between the bearing adapter and the side frame of the truck. The main benefits of implementing the elastomer steering pad on top of the bearing adapter include: improvement of axle-to-rail alignment which allows a controlled motion of the wheelset with reduced lateral force in curves, a wheelset life increase of 25%, and an 8% decrease in fuel consumption, among other benefits [5]. However, the suspension element also acts as an insulator of heat from the adapter to the components in contact above the pad. Moreover, viscoelastic materials, such as the railroad bearing thermoplastic elastomer suspension element (or elastomeric pad), are known to develop self-heating (hysteresis) under cyclic loading, which can lead to undesirable consequences [7]. If there is no thermal runway for the heat to dissipate out of the suspension pad, and the pad is being subjected to abnormal loading frequencies, the internally generated heat is significant and can cause the suspension pad to reach temperatures higher than those of any other component in the truck assembly. Additional work presents the temperature distribution of the thermoplastic elastomer suspension pad (shown in Figure 1) due to the heating of the railroad bearing for both normal and abnormal operation conditions [4]. The results indicate that the adapter pad reaches temperatures of up to 52ºC (assuming an ambient temperature of 25ºC) during normal operation conditions (full load and a train speed of 85 km/h or 53 mph).

The purpose of the work presented in this paper is to investigate the effect of the internal heat generation in the railroad thermoplastic elastomer suspension element on the thermal behavior of the railroad bearing assembly. Understanding the impact of the hysteresis heating of the railroad bearing elastomer suspension element during operation is essential to predict its dynamic response and structural integrity, as well as, to predict the thermal behavior of the railroad bearing assembly. For example, understanding the thermal behavior of the bearing adapter during operation is essential for sensor selection and placement within the adapter (e.g., typical temperature sensors have operating ranges of up to 125°C) [4]. Previous experimental and FEA work indicate that the bearing adapter depicted in Figure 1 can reach temperatures of 68ºC and 120ºC for normal and abnormal operation conditions, respectively [4].

Figure 1. Railroad bearing AdapterPlus™ with elastomer suspension pad [5]

The following sections present an experimentally validated finite element thermal model which can be used to acquire temperature distribution maps of complete bearing assemblies taking into account the hysteresis heating of the railroad bearing elastomer suspension element during normal and abnormal service conditions.

HEAT GENERATION DUE TO HYSTERESIS HEATING

To determine the energy being released by the component, the total heat generation of the material was numerically estimated using dynamic mechanical analysis (DMA) data that were obtained from specimens of the suspension pad material [8]. The data showed that the loss modulus decreases as the specimen temperature increases, meaning that the heat generation would be dependent on temperature. The higher the temperature of the pad, the lower the dissipation of energy as heat [9]. Since the heat generation is a function of the loss modulus, strain percent, and frequency, equation (1) can be used with DMA results to calculate specific power (W/m^3) dissipated at individual frequencies and temperatures.

$$P = \frac{\omega}{2}\varepsilon_A^2 E^{"} \tag{1}$$

For the heat generation calculations, the applied strain of 0.05 cm/cm in the experiments was used in conjunction with the

loss modulus data obtained from the DMA tests. A loading frequency sweep was done on each specimen ranging from 0.1 to 50 Hz; however, heat generation values were calculated only for frequencies of 10, 20, 30, and 50 Hz. The heat generation is also dependent on temperature, and at each frequency, values for the internally generated heat are calculated for temperatures ranging from 30 to 160ºC in increments of 10ºC. Table 1 and Figure 2 display the heat generation values for all frequency ranges dependent on the temperature.

Table 1. Calculated heat generation values

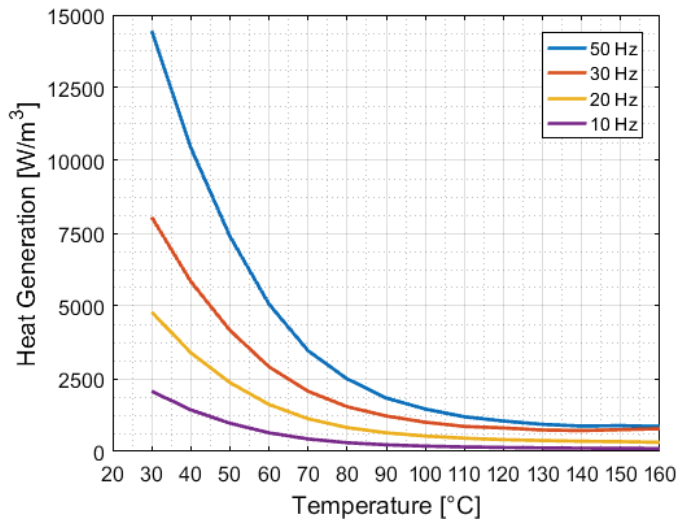| Temperature [°C]	50 Hz Heat Generation [W/m^3]	30 Hz Heat Generation [W/m^3]	20 Hz Heat Generation [W/m^3]	10 Hz Heat Generation [W/m^3]
30	14459	8053	4793	2070
40	10441	5842	3394	1428
50	7397	4165	2369	970
60	5065	2910	1615	641
70	3463	2068	1123	428
80	2493	1537	821	300
90	1836	1219	641	228
100	1457	1004	529	184
110	1191	859	455	155
120	1045	808	405	137
130	931	737	375	121
140	873	716	350	111
150	888	748	338	106
160	860	781	313	100

Figure 2. Heat generation curves at different loading frequencies

EXPERIMENTAL SETUP

The laboratory experiments conducted at UTRGV were performed using two dynamic bearing test rigs, a single bearing tester (SBT) and a four-bearing tester (4BT). The single bearing tester, shown in Figure 3, can apply vertical, lateral (axial), and impact loading on one Class F (6½"×12") or Class K (6½"×9") tapered-roller bearing. The test rig is specifically designed to closely mimic railroad service conditions which a railroad bearing experiences. The vertical load is applied utilizing a hydraulic cylinder capable of applying loads ranging from 0 to 175% of full load. A fully-loaded railcar (100% load) corresponds to an applied load of 153 kN (34.4 kips) per bearing for Class F and Class K bearings, whereas, an empty railcar (17% load) corresponds to an applied load of 26 kN (5.85 kips) [4]. The four bearing tester (4BT), shown in Figure 4, accommodates four of the abovementioned tapered-roller bearings (either Class K or Class F), pressed onto a test axle. The 4BT can only apply vertical loads with similar ranges to those of the SBT using a similar hydraulic cylinder. Both dynamic bearing test rigs use a variable-speed motor powered by a variable-frequency drive (VFD), which simulates train speeds ranging from 5-137 km/h (or 8-85 mph). Forced convection cooling is achieved with two industrial strength fans, as depicted in Figure 4, that produce an average air stream of 18 km/h (11.2 mph). The air stream produced by the fans is meant to simulate the air flow passing across the bearing in field service.

Figure 3. Single Bearing Tester (SBT)

3 Copyright © 2018 by ASME

Figure 4. Four Bearing Tester (4BT)

HEAT TRANSFER FINITE ELEMENT MODELING

This section presents an experimentally validated finite element thermal model that can be used to obtain temperature distribution maps of complete bearing assemblies in service conditions. First, a computer aided design (CAD) model was created and constructed in Solid Works™, which was then imported into ALGOR 20.3™ to create a finite element model for the heat transfer analysis, as seen in Figure 5.

A combination of bricks, wedges, pyramids, and tetrahedral elements were used to successfully mesh the model. The complete laboratory bearing assembly FE model includes a tapered-roller bearing that is pressed onto the axle and assumes that all rollers contribute the same amount of thermal load. The length of the axle accounts for the different thermal runways caused by the insulating properties of the thermoplastic elastomer suspension pad. Some of the boundary conditions as well as the overall heat transfer coefficients were acquired from experimental and theoretical work performed previously and summarized in reference [3]. Four major boundary conditions were applied: conduction, convection, heat flux, and heat generation. Model simplifications were made including the following: no roller cages, seals, wear rings, or grease were included. The thermal resistances of both the grease and the polyamide cages are very large compared to that of the bearing components, and their exclusion is justified in reference [2]. Other assumptions include the contact area of the roller to the cup (outer ring) and cone (inner ring) raceways and the thermal contact resistance between the bearing cup and the adapter. Since the roller-cone and roller-cup contact areas change whenever the bearing is loaded or unloaded, and during normal operation

conditions only the upper hemisphere of the bearing is loaded, larger contact areas exist in this region. Hence, an average value for the roller-cup and roller-cone contact area was applied to each one of the 46 rollers in the bearing assembly [2]. It is important to note that, since this is a static model, the actual rotation of the cone assemblies inside the bearing was not directly simulated, but was taken into account by applying an average heat flux through all 46 rollers in the bearing [4]. Thermal contact resistance between the bearing cup and the adapter can significantly affect the amount of heat transferred to the bearing adapter. Consequently, this contact resistance can dictate the temperature difference between the two components. Values for the contact pressure between the cup and adapter were obtained based on several pressure film experiments. A detailed description of this methodology is provided elsewhere [4].
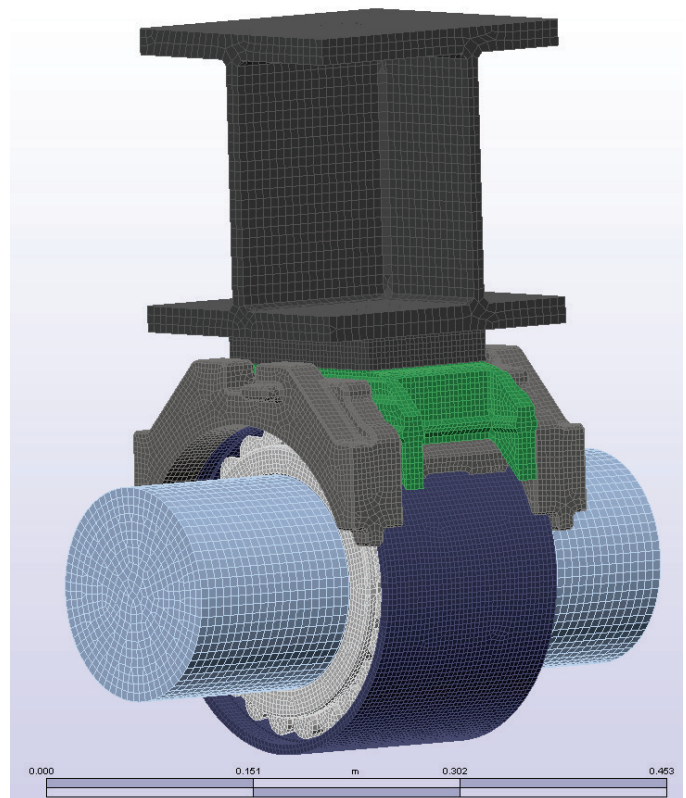

Figure 5. Complete laboratory bearing assembly FEA model

Material properties for the bearing components, axle, I-beam, spacer ring, adapter, and spacer plate were all directly selected from ALGOR 20.3™. For the bearing components, AISI 8620 steel with a thermal conductivity of 49.3 $W \cdot m^{-1} \cdot K^{-1}$ was used; for the axle, I-beam, spacer ring, and spacer plate, AISI 1050 steel with a thermal conductivity of 51.9 $W \cdot m^{-1} \cdot K^{-1}$ was used, further detailed descriptions are provided in reference [4]. For the adapter pad, properties of the specimen material were sourced from BASF literature on thermoplastic polyurethane (TPU) using data from material grades with the same shore durometer value. A thermal conductivity of 0.25 $W \cdot m^{-1} \cdot K^{-1}$ along with a mass density of 1160 $kg \cdot m^{-3}$ and a specific heat of

2.3 $J \cdot g^{-1} \cdot K^{-1}$ were selected as the specific properties. Ductile (nodular) iron with a thermal conductivity of 34.4 $W \cdot m^{-1} \cdot K^{-1}$ was used for the bearing adapter material. Table 2 obtained from reference [4] lists the convection coefficient values for all the FE model components.

Table 2. Convection coefficient values for each FE model component

Part	h_{avg} [$W \cdot m^{-2} \cdot K^{-1}$]
I-beam	19.0
Spacer Plate	18.3
AdapterPlus™	17.9
Adapter Pad	17.9
Overall Average	18.1

The convection boundary condition for the bearing cup was obtained from previous theoretical and experimental work presented in references [2] and [3]. An overall heat transfer coefficient H_o = 8.32 $W \cdot K^{-1}$ is provided for the bearing cup, taking into account the forced convection that is generated by the average air flow of 5 m/s and radiation to the ambient air at a temperature of 25ºC. However, the software appropriate units require the aforementioned convection value to be divided by the bearing cup surface area (A_{cup} = 0.1262 m^2), leading to a cup convection coefficient h_o = 65.9 $W \cdot m^{-2} \cdot K^{-1}$.

For the axle, the convection coefficient was obtained by using the Nusselt number correlation for a cylinder in cross-flow. A resulting value of h_{axle} = 25 $W \cdot m^{-2} \cdot K^{-1}$ is obtained from reference [4]. For the adapter, adapter pad, I-beam, and spacer plate, the convection coefficient values were obtained by using the Nusselt number correlation for a flat plate in parallel flow. Table 2 obtained from reference [4] lists the convection coefficient values for all the model components.

The work reported in reference [2] indicates that the total heat input needed to generate a cup temperature of 50°C is about 529 W per bearing. From the same reference, the power required to produce a cup temperature of approximately 72°C (indicating abnormal operation) is 980 W [2]. For simplicity, the heat flux was only applied to the surface of the rollers; i.e. 11.5 W per roller for normal operation, and 21.3 W per roller for abnormal operation. Here, it is assumed that the rollers are the source of heat within the bearing which is justified considering the mass of the roller (0.145 kg) relative to the mass of the bearing cup (11.53 kg) and cone (3.9 kg). Since the mass of the roller is very small compared to the mass of the cup and cone, it is safe to assume that it will heat at a much faster rate than the other two components, thus, becoming the heat source [2].

Another heat source or thermal mechanism boundary condition is the hysteresis heat generation that is produced by the thermoplastic elastomer suspension element. Previous studies show that an applied constant heat generation at high loading frequencies such as 50 Hz in combination with high ambient temperatures and no thermal runway can propel elastomer suspension pad temperatures significantly above the softening

temperature of the pad material (i.e. 120ºC) [7]. The heat generation applied to the adapter pad is a constant heat generation for frequency loadings of 10 and 50 Hz, which simulate a defect-free and defective bearing assembly in the laboratory, respectively. The heat generation is applied to both normal and abnormal condition models.

Thermal contact resistance between the adapter and bearing cup may significantly affect the amount of heat transferred to the bearing adapter. Values for the contact resistance were obtained from a pressure film study explained in reference [4]. A thermal contact resistance of 0.0055 $m^2 \cdot K \cdot W^{-1}$ was applied in between the bearing cup and adapter. Consequently, in order to model both heat sources simultaneously (i.e. the heat flux of the rollers and the heat generation of the suspension pad), a thermal contact resistance of 0.01 $m^2 \cdot K \cdot W^{-1}$ was applied between the suspension pad and the metal adapter, and between the suspension pad and the I-beam spacer plate. Figure 6 displays the complete FE model with the convection and heat flux boundary conditions applied to each individual component.

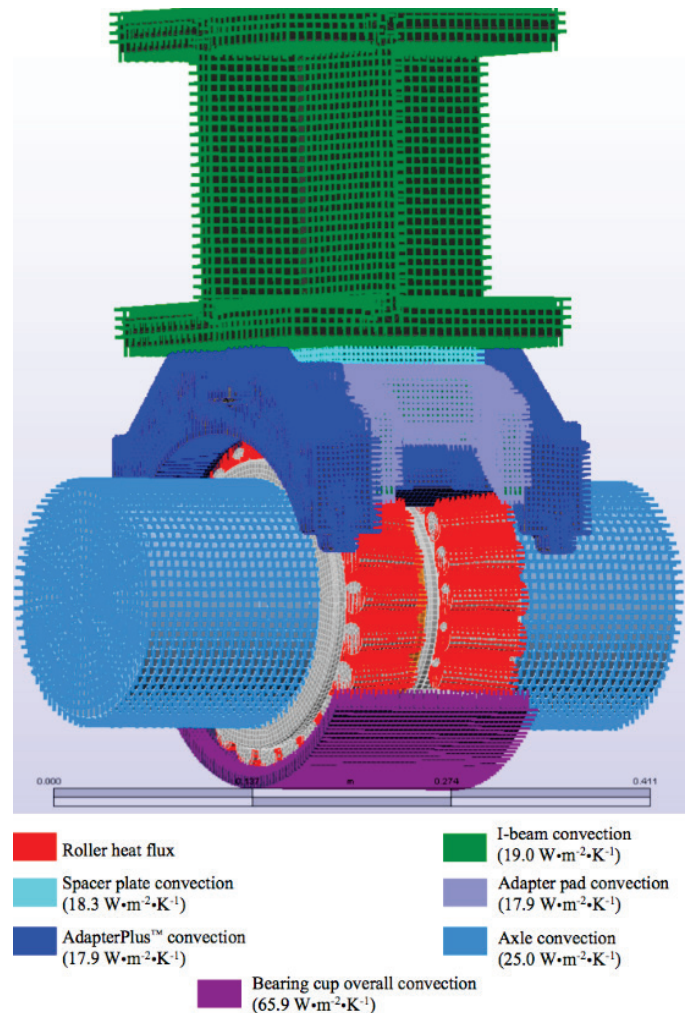| Roller heat flux | I-beam convection (19.0 $W \cdot m^{-2} \cdot K^{-1}$) |
Spacer plate convection (18.3 $W \cdot m^{-2} \cdot K^{-1}$)	Adapter pad convection (17.9 $W \cdot m^{-2} \cdot K^{-1}$)
AdapterPlus™ convection (17.9 $W \cdot m^{-2} \cdot K^{-1}$)	Axle convection (25.0 $W \cdot m^{-2} \cdot K^{-1}$)
Bearing cup overall convection (65.9 $W \cdot m^{-2} \cdot K^{-1}$)	

Figure 6. Boundary conditions applied to each FE model component

Table 3 displays the parameters of the experimental tests chosen for comparison. Both normal and abnormal laboratory conditions were applied to the models.

Table 3. Laboratory operation conditions for FEA comparison

Operation Condition	Ambient Temp. [°C]	Load [%]	Train Speed [km/h] / [mph]
Normal	25	100	96.6 / 60
Abnormal	45	100	137 / 85

FINITE ELEMENT ANALYSIS

The finite element (FE) model thermal maps presented in reference [4] were used as the basis for the thermal maps presented in this paper. The initial step was to replicate the experimental results presented in reference [4]. Figure 7 displays the FE model with markers showing the location of the selected nodes. The same reference temperature locations on the adapter were used for comparison and model validation. Using the boundary conditions and modeling methods explained in the previous section and summarized in Figure 6, the preliminary results shown in Figure 8 were obtained. Once it was determined that the results of the complete FE model developed for this study matched the experimental results acquired from reference [4], a second simulation scenario was modeled with the inclusion of the heat generation produced by the thermoplastic elastomer suspension pad.
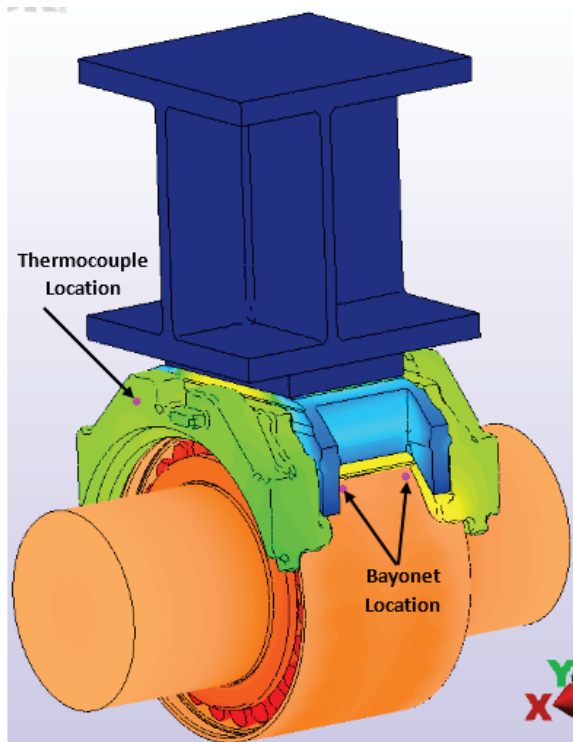
Figure 7. AdapterPlus™ FE model with nodes of interest indicated
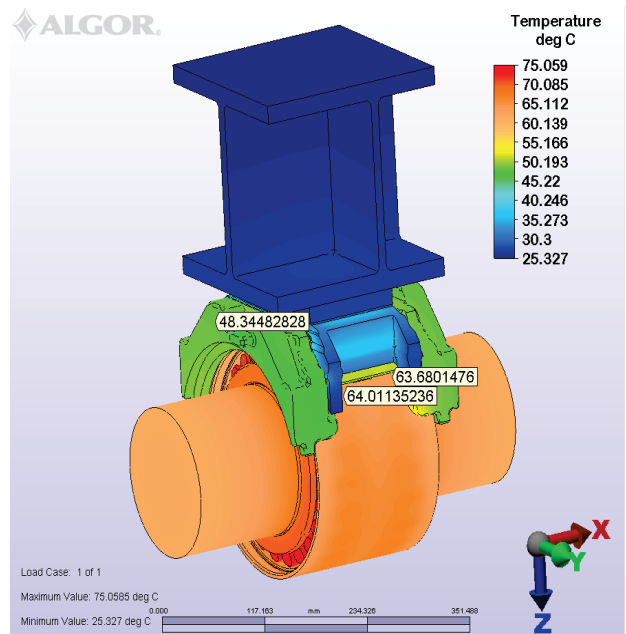
Figure 8. Temperature distribution with normal operation conditions and no heat generation

FEA Laboratory Results Validation

A temperature map of the complete bearing assembly for normal operation conditions, displayed in Figure 8, was obtained as a result of the thermal finite element analysis (FEA) conducted utilizing the newly developed FE model. Table 4 provides a comparison between the results of the simulation of Figure 8 and the experimental temperature data acquired through dynamic testing. The comparison indicates a maximum temperature difference of no more than 9.5% in the thermocouple location indicated on the adapter of Figure 7. In the bayonet locations, the average temperature difference was only about 2%. This small difference demonstrates the efficacy of the model, and validates all of the assumptions and boundary conditions that were used to devise this new FE model.

Table 4. Experimental and FEA results comparison

Normal Operation Conditions		
Source of Results	**Thermocouple [°C]**	**Bayonet [°C]**
Experimental	44.2	65.4
FEA	48.4	64.1
% Difference	9.5	2

For the simulation presented in Figure 8, the suspension elastomer pad partially insulates the I-beam from the bearing assembly reducing its ability to act as a heat sink. Since heat tends to transfer through the path of least resistance, most of the heat will be conducted through the axle rather than the I-beam, which justifies the axle length chosen for this FE model.

A temperature map of the AdapterPlus™ elastomer suspension pad was also obtained through FEA. Figure 9 and Figure 10 provide, respectively, the bottom and top surface temperature maps of the suspension pad during normal operation conditions. The figures demonstrate that most of the heat from the adapter is dissipated by convection along the sides of the adapter, while significantly less heat is dissipated by conduction through the central rectangular area on the bottom surface of the suspension pad. The latter becomes apparent when comparing the temperatures of the bottom and top surfaces of the elastomer suspension pad (refer to Figure 9 and Figure 10). It is evident that most of the heat is partially insulated from the I-beam and spacer plate. The temperature map of the thermoplastic elastomer suspension pad was obtained for normal operation conditions and was compared to that of previous studies [4]. The study concluded that the bottom surface of the suspension pad experiences the highest temperatures reaching about 50ºC, which can be seen from Figure 9.
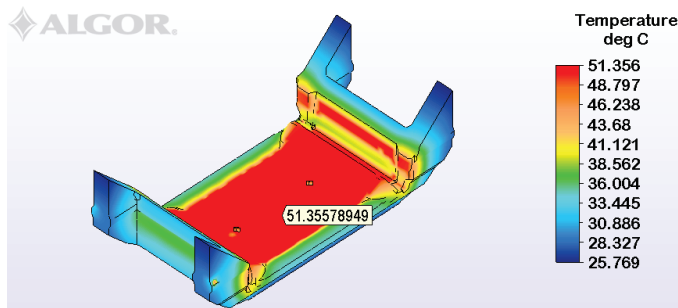
Figure 9. Bottom surface temperature distribution and maximum temperature of the suspension pad with normal operation conditions
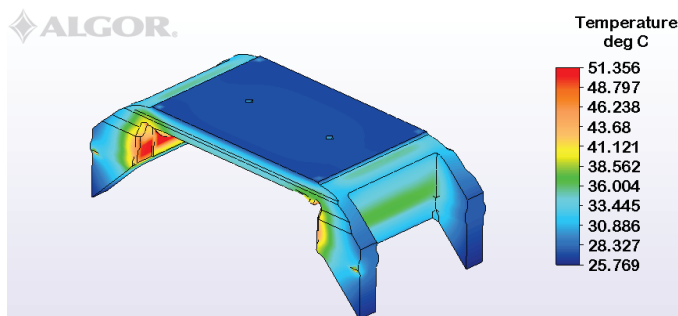
Figure 10. Top surface temperature distribution of the suspension pad with normal operation conditions

FEA Modeling with Suspension Pad Heat Generation for Normal Operation Conditions

Figure 11 presents the temperature map of the AdapterPlus™ FE model when a constant heat generation due to a loading frequency of 10 Hz is applied. When compared to the simulation results presented in Figure 8, the results in Figure 11 show almost no change in the temperature distribution of the bearing assembly, adapter, or suspension pad. Table 5 provides the temperature difference of the locations of interest (refer to Figure 7) between the two different model simulations.
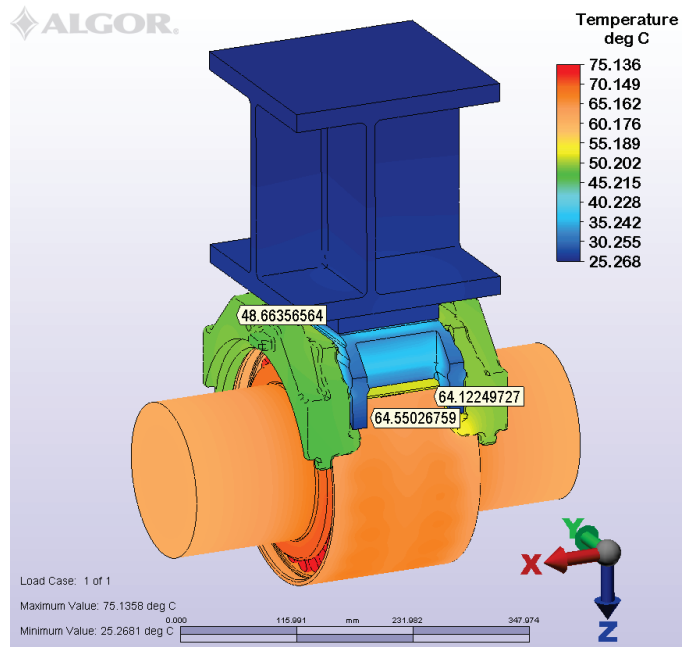

Figure 11. AdapterPlus™ FE model with an applied heat generation due to a frequency loading of 10 Hz and normal operation conditions

Table 5. AdapterPlus™ FE model temperature comparison (no pad heat generation versus 10 Hz pad heat generation)

Normal Operation Conditions			
Operation Condition	Bayonet [°C]	Thermocouple [°C]	Pad [°C]
Heat Generation	64.4	48.9	51.6
No Heat Generation	64.1	48.4	51.4
ΔT [°C]	0.3	0.5	0.2

Figure 12 and Figure 13 provide, respectively, the bottom and top surface temperature maps of the suspension pad during normal operation conditions with an applied heat generation due to a loading frequency of 10 Hz. Although the maximum pad temperature is nearly the same for the two simulations (i.e. with and without pad heat generation), the temperature distribution within the pad differs markedly. Comparing the two simulations, it can be observed that the maximum temperature at the bottom surface shifts from the center of the pad (Figure 9) to the pad interlocks (Figure 12). Moreover, the temperature of the top surface of the pad is warmer for the simulation with pad heat generation (Figure 13) compared to the simulation with no pad heat generation (Figure 10).
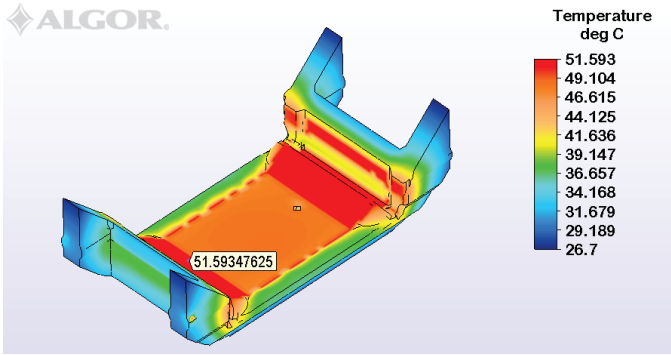
Figure 12. Bottom surface temperature distribution and maximum temperature of the suspension pad with normal operation conditions and an applied constant heat generation due to a frequency loading of 10 Hz
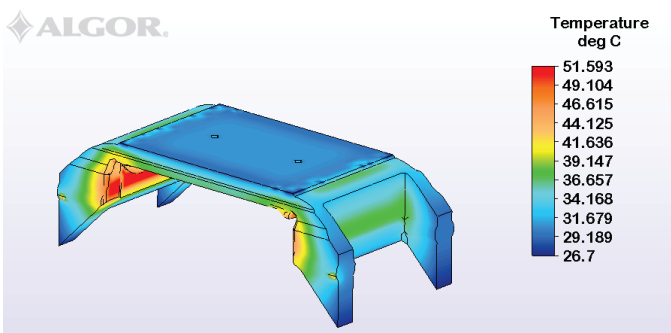

Figure 13. Top surface temperature distribution of the suspension pad with normal operation conditions and an applied constant heat generation due to a frequency loading of 10 Hz
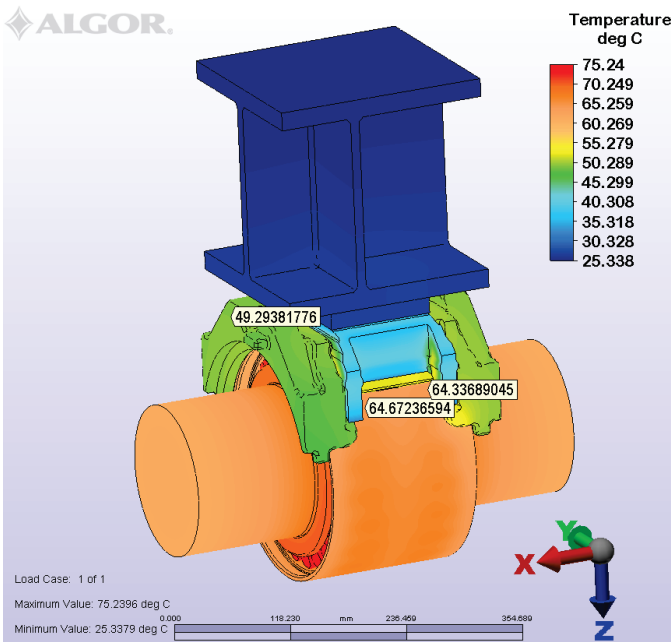

Figure 14. AdapterPlus™ FE model with an applied heat generation due to a frequency loading of 50 Hz and normal operation conditions

Figure 14 gives the temperature map of the AdapterPlus™ FE model when a constant heat generation due to a loading frequency of 50 Hz is applied. The results of this simulation compared to those in Figure 8 and Figure 11 show that the higher applied pad heat generation hardly affects the temperature distribution of the bearing assembly or the adapter. However, the temperature distribution of the suspension pad is affected. Figure 15 shows that the maximum temperature of the pad increases by 4°C, and the region of maximum temperature at the bottom surface of the pad shifts to the pad legs. Table 6 displays the temperature difference between the model with no applied heat generation in the suspension pad and the model with an applied constant heat generation due to a frequency loading of 50 Hz.
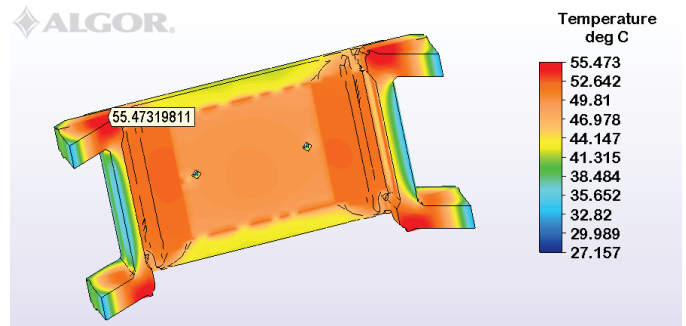

Figure 15. Bottom surface temperature distribution and maximum temperature of the suspension pad with normal operation conditions and an applied constant heat generation due to a frequency loading of 50 Hz

Table 6. AdapterPlus™ FE model temperature comparison (no pad heat generation versus 50 Hz pad heat generation)

Normal Operation Conditions			
Operation Condition	Bayonet [°C]	Thermocouple [°C]	Pad [°C]
Heat Generation	64.5	49.3	55.5
No Heat Generation	64.1	48.4	51.4
ΔT [°C]	0.4	0.9	4.1

FEA Modeling with Suspension Pad Heat Generation for Abnormal Operation Conditions

Figure 16 presents the temperature distribution map of the AdapterPlus™ FE model with abnormal operation conditions and no applied pad heat generation. The figure shows a significantly higher overall temperature distribution for the system, which is mainly due to the increased roller heat flux and ambient temperature. Figure 17 and Figure 18 provide the temperature distribution of the models with applied pad heat generation of 10 and 50 Hz, respectively. Interestingly, the temperature distribution results for the models with applied heat generation due to frequency loadings of 10 and 50 Hz do not exhibit a significant increase in temperature at the locations of interest compared to the model with no applied heat generation presented in Figure 16, as summarized in Table 7.
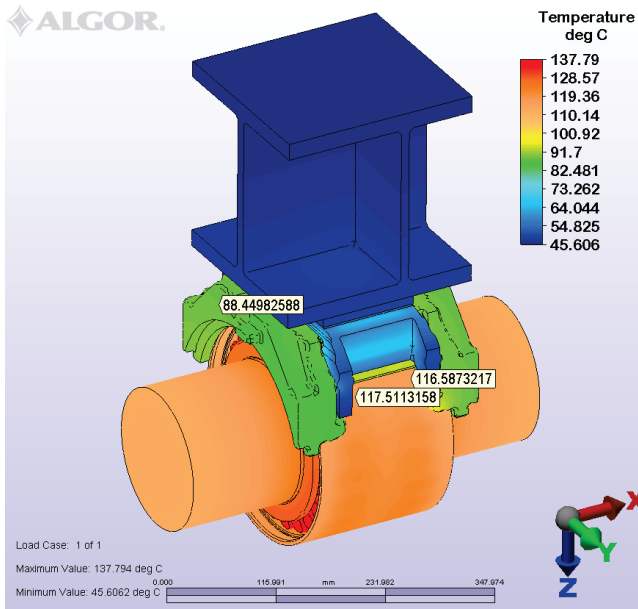
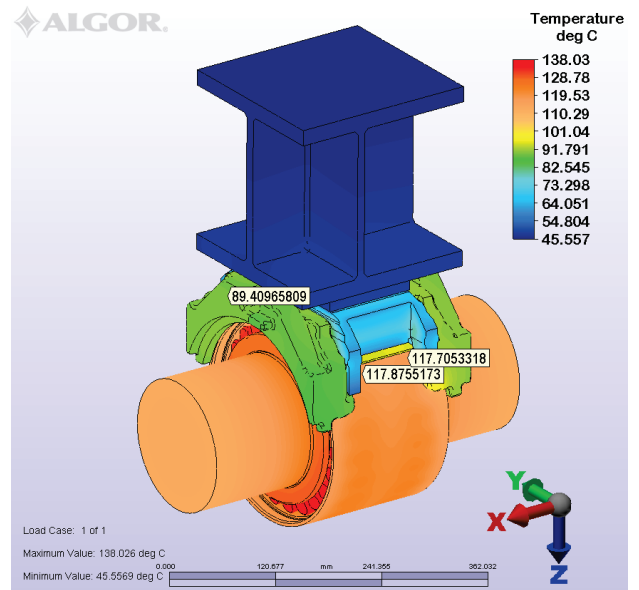Figure 16. AdapterPlus™ FE model with abnormal operation conditions and no applied pad heat generation

Figure 17. AdapterPlus™ FE model with an applied heat generation due to a frequency loading of 10 Hz and abnormal operation conditions
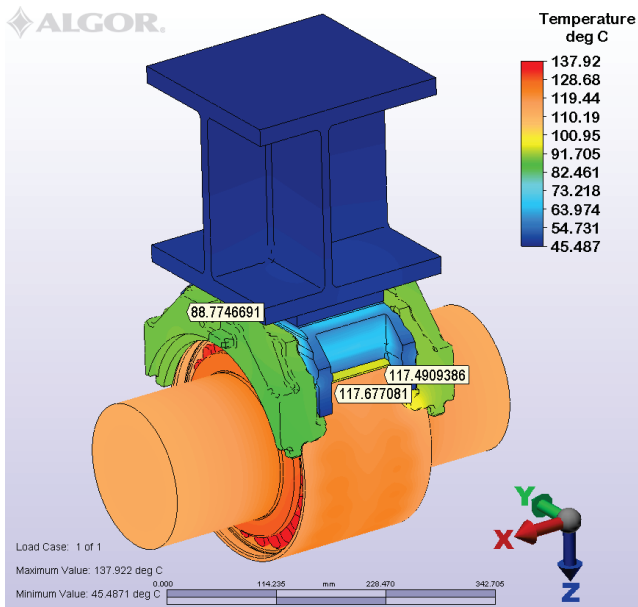
Table 7. AdapterPlus™ FE model temperature comparisons

Abnormal Operation Conditions			
Applied Pad Heat Generation	Bayonet [°C]	Thermocouple [°C]	Pad [°C]
None	117.1	88.4	93.9
10 Hz Loading	117.7	88.8	94.2
50 Hz Loading	117.8	89.4	95.0
Maximum ΔT [°C]	0.7	1.0	1.1

Figure 18. AdapterPlus™ FE model with an applied heat generation due to a frequency loading of 50 Hz and abnormal operation conditions
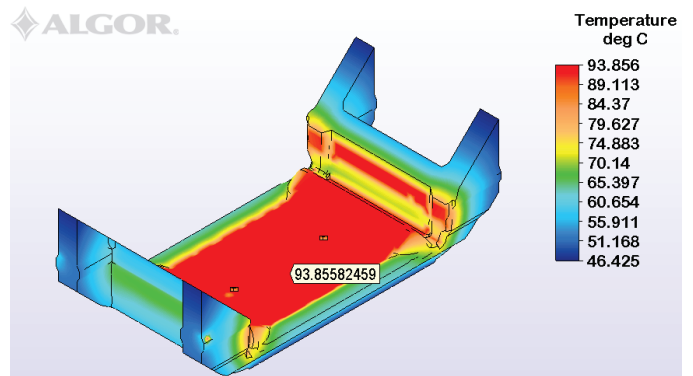

Figure 19. Bottom surface and maximum temperature of the suspension pad with abnormal operation conditions and no applied pad heat generation
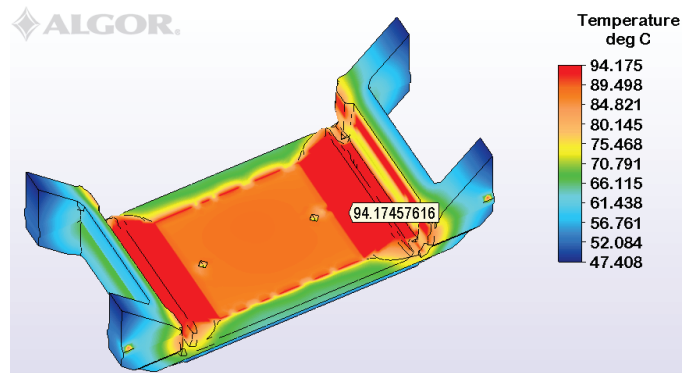

Figure 20. Bottom surface and maximum temperature of the suspension pad for abnormal operation conditions with applied heat generation due to a frequency loading of 10 Hz

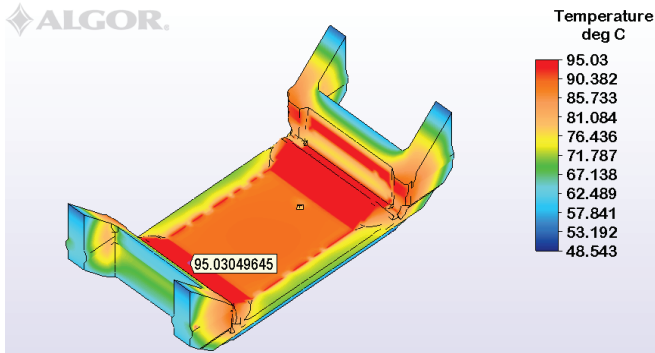9   Copyright © 2018 by ASME

Figure 21. Bottom surface and maximum temperature of the suspension pad for abnormal operation conditions with applied heat generation due to a frequency loading of 50 Hz

Figure 19, Figure 20, and Figure 21 display the abnormal operation condition temperature distribution along with the maximum surface temperature of the suspension pad for the model with no heat generation applied to the pad, the model with an applied heat generation due to a frequency loading of 10 Hz, and the model with an applied heat generation due to a frequency loading of 50 Hz, respectively. Again, the temperature maps clearly demonstrate the shift in the location of maximum temperature within the bottom surface of the suspension pad, described earlier. Table 7 provides a summary of the temperatures of the locations of interest for each of the models.

CONCLUSIONS

An experimentally validated AdapterPlus™ FE model was devised to investigate the effect of elastomer pad hysteresis heating on the railroad bearing assembly operating temperature. Different internal heating scenarios are simulated with the purpose of obtaining the bearing suspension element and bearing assembly temperature distribution maps during normal and abnormal operation conditions along with no heat generation and applied heat generation in the thermoplastic elastomer suspension element.

The results show that in normal and abnormal operation conditions, the internal heat generation in the thermoplastic elastomer suspension element has limited impact on the thermal behavior of the railroad bearing assembly as long as the pad is able to dissipate heat through the side frame of the truck. In fact, previous results show that a combination of the ambient temperature, bearing temperature, and frequency of loading can produce elastomer pad temperature increases above ambient of up to 125ºC when no thermal runway is present.

The AdapterPlus™ FE model also shows that with normal operation conditions the temperature distribution of the suspension pad remains relatively the same when heat generation is applied. However, the constant heat generation due to a frequency loading of 50 Hz does cause the maximum temperature of the pad to increase by about 4°C.

Although this minor increase in temperature is not significant to the temperature distribution of the suspension pad

nor does it significantly impact the thermal management or temperature distribution of the bearing assembly, the results indicate that if a significant amount of energy is generated by the suspension pad with no thermal runway, it can highly impact the structural integrity of the suspension pad.

ACKNOWLEDGMENTS

REFERENCES

[1] 2.09 - Train Accidents and Rates | Federal Railroad Administration, Office of Safety Analysis. Web. safetydata.fra.dot.gov/OfficeofSafety/publicsite/query/TrainAccidentsFYCYWithRates.aspx.

[2] Tarawneh, C., et al. "Thermal Modeling of a Railroad Tapered-Roller Bearing Using Finite Element Analysis." *Journal of Thermal Science and Engineering Applications*, vol. 4, no. 3, pp. 9-19, 2012.

[3] Tarawneh, C., Cole, K., Wilson, B.M., Alnaimat, F., "Experiments and Models for the Thermal Response of Railroad Tapered-Roller Bearings," *International Journal of Heat and Mass Transfer*, Vol. 51, pp. 5794-5803, 2008.

[4] Zagouris, A., Fuentes, A. A., Tarawneh, C., Kypuros, J. A., and Arguelles, A. P., "Experimentally Validated Finite Element Analysis of Railroad Bearing Adapter Operating Temperatures," *Proceedings of the 2012 ASME IMECE Conference*, IMECE2012-88639, Houston, TX, November 9-15, 2012.

[5] Adapter Plus Steering Pad System | Amsted Rail. Web. http://www.amstedrail.com/adapter-plus-steering-pad-system

[6] Ramkumar, A., Kannan, K., and Gnanamoorthy, R., "Experimental and Theoretical Investigation of a Polymer Subjected to Cyclic Loading Conditions," *International Journal of Engineering Science*, Vol. 48: 101-10, 2010.

[7] Rodriguez, O. O., et al. "Hysteresis Heating of Railroad Bearing Thermoplastic Elastomer Suspension Element," *Proceedings of the 2017 ASME Joint Rail Conference,* Philadelphia, PA, April 4-7, 2017.

[8] Rodriguez, O. O., Carbone, J., Fuentes, A. A., Jones, R. E., and Tarawneh, C, "Heat Generation in the Railroad Bearing Thermoplastic Elastomer Suspension Element," *Proceedings of the 2016 ASME Joint Rail Conference*, Columbia, SC, April 12-15, 2016.

[9] Lakes, R. S. Viscoelastic Solids. Boca Raton: CRC, 1999.

[10] Logan, D. L. A First Course in the Finite Element Method. Pacific Grove, CA: Brooks/Cole, 2002.

[11] Incropera, F.P., Dewitt, D.P., Bergman, T.L., Lavine, A.S., *Fundamentals of Heat and Mass Transfer*. Sixth Edition, 2007, Hoboken, NJ: John Wiley & Sons, Inc.